Required screw length measurement in distal tibia based on three-dimensional simulated screw insertion

Kun Zhang, Yanxi Chen*, Minfei Qiang

Department of Orthopaedic Trauma, East Hospital, Tongji University School of Medicine, 150 Jimo Rd, Shanghai 200120, China

Received 1 March, www.tsi.lv

Abstract

The objective of the study was to provide morphological data of the distal tibia to offer guidance on the required screw length. Computed tomography scans of the ankle in 225 patients were reviewed. Then parameters in the three-dimensional reconstruction images were measured by three independent, qualified observers on 2 separate occasions. The anteroposterior length increases from medial to lateral margin at the level of the base of the tibiofibular syndesmosis. On both proximal and distal planes of tibiofibular syndesmosis, the medial-lateral width increases from posterior to anterior margin. Significant differences were observed in all parameters between male and female and in the minimum width at the level of the roof of the syndesmosis between left and right limbs (P<0.05). All of the parameters exhibited moderate to excellent intra-class correlation coefficient. The anteroposterior screws would probably penetrate the far cortex and injure the structures surrounding the distal tibia if longer than 35.35 mm and 32.53 mm in male and female. The screws should not longer than the maximum diagonals which are 51.29 mm and 46.58 mm on distal plane and 43.64 mm and 38.24 mm on proximal plane in male and female respectively, or inadvertent distal tibiofibular syndesmosis penetration may occur.

Keywords: Tibia, Tibiofibular syndesmosis, Tomography, X-ray computed, Imaging, three-dimensional

1 Introduction

Distal tibia fracture is one of the most common lower limb fractures as it is contained in both intra-articular and extra-articular fractures such as metaphyseal and pilon fractures [1-3]. The directions of the screws in distal tibia are flexible and should be determined by different types of plates and the pattern of fracture lines [4-8]. Sometimes length determined by depth gauge is imprecise in distal tibia, especially when the far cortex is fragmentized in tibiofibular syndesmosis. The screws inserted may be too long or too short. Then the screws should be replaced and more fluoroscopy is inevitable. The more frequent the fluoroscopy was used, the more radiation exposure surgeons and patients will receive [9]. Therefore, it is important for surgeons to understand the morphology of the distal tibia in all directions.

As more and more orthopaedic surgeons tried to treat distal tibia fracture with minimally invasive plate osteosynthesis (MIPO) [4-8], complications associated with this technique have been described and included infection, damage to neurovascular structures and bone and tendon impingement [10, 11]. Previous studies demonstrated that key anatomical structures including neurovascular bundles and tendons are in very close proximity to the distal tibia [11, 12]. Furthermore, only a small gap exists in the distal tibiofibular syndesmosis [5, 13, 14]. Frequent use of depth gauge, percutaneous insertion and replacement of screws, and poor implantation may lead to injury to nerves, vessels, tendons and articular surfaces. Exposed screw tail may stimulate and injure adjacent anatomic structures. Therefore, there is little room for error treating distal tibia fractures and extreme caution should be exercised. Knowledge of the distal tibia morphology in all directions may help to decrease the possibility of key anatomical structure damage and inadvertent tibiofibular syndesmosis penetration. However, scarce data are available concerning the morphology of the distal tibia.

The objective of the study was to provide morphological data of the distal tibia to offer guidance on the required screw length in all directions.

2 Materials and Methods

2.1 SUBJECTS

Institutional ethical approval for this study was obtained from the Ethics Committee of our hospital, and conforms to the provisions of the Declaration of Helsinki. (East Hospital Ethics Committee, Ethics number 2012-020). The patients were collected from the foot and ankle clinic of our hospital and informed consent was obtained. Patients were excluded if they had a history of distal tibia fracture, pilon fracture, internal or posterior malleolus fracture confirmed by radiological examination or surgery. Patients with congenital or acquired malformation, osteoarthritis, rheumatoid arthritis or a history of bone tumour of ankle were also excluded.

**Corresponding author* e-mail: cyxtongji@126.com

Patients less than 20 years old or older than 65 years were excluded to avoid skeletal immaturity or degeneration. Finally, 225 patients were enrolled in this study, with 122 men (with 122 ankle joints) and 103 women (with 103 ankle joints). There were 104 left and 121 right ankle joints. The average age was 39.5 years (range, 20 to 65 years).

2.2 IMAGE ACQUISITION AND POST PROCESSING

The thin-slice CT images (DICOM 3.0 format) of all the patients scanned by 16-row spiral CT (Light Speed, GE, USA) were collected. Main CT scanning parameters were as follows: thickness, 0.625 mm; voltage, 120 kV; current, 200 mA; image matrix, 512×512.

The thin-slice CT axial images of all research subjects were firstly uploaded to picture archiving and communication system (PACS) of hospital, then these CT data were imported into the digital orthopaedic clinical research platform (SuperImage orthopaedics edition 1.0, Cybermed Ltd, Shanghai, China) via removable storage devices. On this platform, three-dimensional (3-D) images of ankle joints were generated by performing surface shaded display with a bone algorithm at 0.625 mm slice thickness. All component bones of ankle joints were distinguished by computer in 3-D images. Then parameters in the 3-D reconstruction images could be measured and calculated.

2.3 MEASUREMENTS AND CALCULATIONS

Design of the parameters in distal tibia closely combined clinical experiences. The trajectories which were most commonly used in distal tibia were visualized by inserting simulated screws (Figure 1, 2). In order to standardize the measurement process so that other researchers could replicate the study, we designed the steps below.

Firstly, on the distal tibia articular surface, the turning point of posterior malleolus and medial malleolus (point A), the turning point of medial malleolus and anterior ankle (point B) and the peak of the lateral margin of the tibial plafond (point C) were selected to define the cross-section (plane ABC) which was corresponded to the most distal slice at the level of the plafond as well as the base of the distal tibiofibular syndesmosis (Figure 3).

Secondly, on the cross-section ABC, points were randomly selected in the antero-medial, antero-lateral, postero-medial and postero-lateral arcs (point E, F, G and H, respectively). The midpoint of the medial margin (point D) and the point in the most front of the anterior margin (point I) were also selected. The distances between point G and E, between point A and B and between point H and I were measured and analysed to obtain the anteroposterior lengths. The distances between point D, E, G and point C, F, H were measured respectively (line DC, DF, DH, EC, EF, EH, GC, GF and GH) and analysed to obtain the medial-lateral widths and diagonal distances (Figure 3).

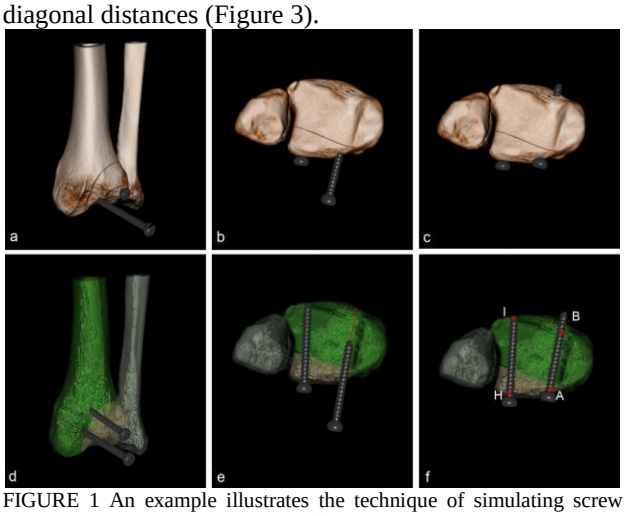

FIGURE 1 An example illustrates the technique of simulating screw insertion and clinical application of the anteroposterior length. (a) A posterior malleolar fracture was simulated in 3-D volume rendering mode. After reduction of the fracture, two screws were simulated to fix the fragment. A screw was inserted and the other to be inserted. (b) A screw was being inserted into the trajectory. (c) After insertion, the figure revealed that the left screw was appropriate and the other was too long. (d-f) The same simulation in surface shaded display mode, which corresponds to Figure 2a-c. (e) The perspective figures revealed the inner part of the tibia. The red arrow was the trajectory. (f) The distance between point A and B and between H and I presented the proper length of the screw. The right screw was too long and penetrated the far cortex.

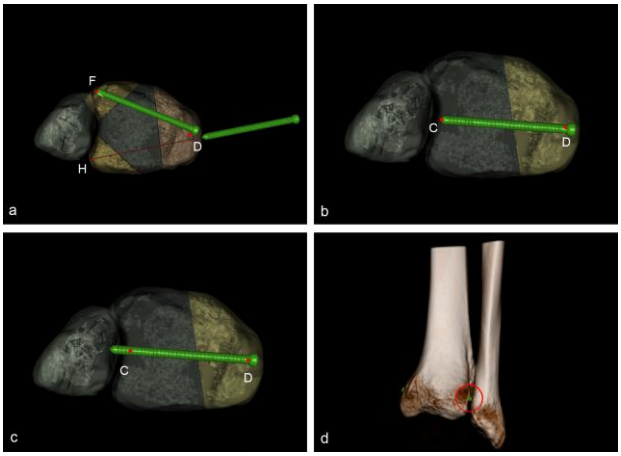

FIGURE 2 An example of clinical application of the medial-lateral width of the distal tibia. The distance between point D and H, between D and F (a) and between D and C (b) presented the proper length of the screw. (c) The figure revealed that the screw was too long and the far cortex was penetrated. (d) The tibiofibular syndesmosis penetration of the screw (marked with red circle) could be observed clearly in volume rendering mode.

Next, plane J was determined through the most proximal point of the anterior tubercle of the distal tibia as the roof of the distal tibiofibular syndesmosis, which is parallel to the plane ABC (Figure 4).

Finally, on this profile, points were randomly selected in the antero-medial, antero-lateral, postero-medial and postero-lateral arcs (point M, N, O and P). The midpoints of medial and lateral margins (point K and L) were also selected. The distances between point K, M, O and point L, N, P were measured respectively (line KL, KN, KP, ML, MN, MP, OL, ON and OP) and analysed to obtain

the medial-lateral widths and diagonal distances (Figure 4).

The measurements were performed on 2 separate occasions by 3 independent, qualified observers. All observers were blinded to the other's analysis. The average was taken as the final data.

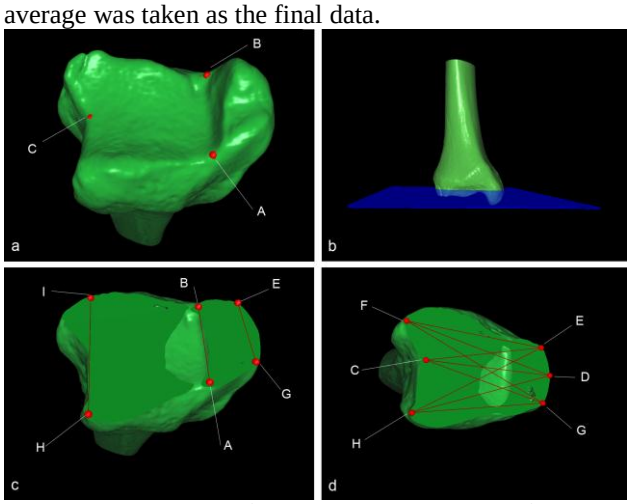

FIGURE 3 Measurement of the distal tibia. (a, b) Base of the distal tibiofibular syndesmosis (plane ABC) was defined by selecting three anatomical landmarks (point A, B and C). (c) Three lines (line GE, AB and HI) were measured and analysed to obtain the anteroposterior lengths. (d) Measuring 9 lines (line DC, DF, DH, EC, EF, EH, GC, GF and GH) to obtain the medial-lateral widths and the maximum distance.

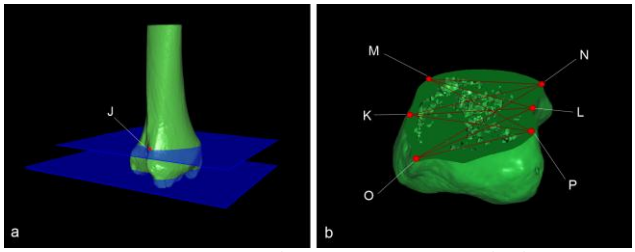

FIGURE 4 The dimension of the tibia on the roof of the distal tibiofibular syndesmosis. (a) Cross-section J was determined through the most proximal point (point J) of the anterior tubercle of the distal tibia. (b) Obtain the medial-lateral width and the maximum distance by measuring 9 lines (line KL, KN, KP, ML, MN, MP, OL, ON and OP).

2.4 STATISTICAL ANALYSIS

SPSS 18.0 (SPSS Inc, Chicago, IL, USA) was used for statistical analysis. The parameters between male and female, and between left and right limbs were compared using the two-samples t test. The lengths and widths were analyzed using the one-way ANOVA. The intra-class correlation coefficient (ICC) was used to assess intraobserver and interobserver reliability. $P<0.05$ was considered to be statistically significant.

3 Results

The mean dimensions of the distal tibia were 41.37 ± 3.22 mm (line DC, range 35.32-49.47 mm, 95% confidence interval [CI]: 40.67-42.11) medial-lateral and 23.83 ± 2.12 mm (line AB, range 20.10-30.47 mm, 95% confidence interval [CI]: 23.45-24.23) anteroposterior at the level of the base of the distal tibiofibular syndesmosis and 35.49 ± 3.29 mm (line KL, range 27.72-45.20 mm, 95% confidence interval [CI]: 34.75-36.24) medial-lateral at the level of the roof of the syndesmosis.

At the level of the base of the syndesmosis (plane ABC), the anteroposterior length increases from medial to lateral margin. The minimum anteroposterior length of distal tibia was 19.14 ± 1.79 mm (line GE, range 15.28-23.60 mm, 95% confidence interval [CI]: 18.82-19.50) and the maximum was 34.09 ± 2.47 mm (line HI, range 27.57-38.88 mm, 95% confidence interval [CI]: 33.63-34.57). The medial-lateral width increases from posterior to anterior margin. The minimum and maximum widths were 38.29 ± 3.39 mm (line GH, range 31.27-46.25 mm, 95% confidence interval [CI]: 37.59-39.04) and 45.36 ± 3.66 mm (line EF, range 38.28-54.43 mm, 95% confidence interval [CI]: 44.56-46.18), respectively.

At the level of the roof of the syndesmosis (plane J), the medial-lateral width increases from posterior to anterior margin. The minimum width was 30.28 ± 3.67 mm (line OP, range 22.98-38.78 mm, 95% confidence interval [CI]: 29.50-31.12), and the maximum was 35.94 ± 3.09 mm (line MN, range 30.20-41.85 mm, 95% confidence interval [CI]: 35.27-36.66).

The longest distance on both planes were diagonals from postero-medial to antero-lateral arc which were 49.01 ± 3.57 mm (line GF, range 41.43-57.13 mm, 95% confidence interval [CI]: 48.19-49.82) on plane ABC and 41.04 ± 4.25 mm (line ON, range 30.18-49.08 mm, 95% confidence interval [CI]: 40.06-42.07) on plane J.

Significant differences were observed in all parameters between male and female (Figure 5), and in the minimum width on the cross-section J between left and right limbs ($P<0.05$) (Figure 6).

Table 1 shows the reliability of all parameters and the intra-observer reliability between three observers.

4 Discussion

Because of the difficulty in defining coronal, sagittal and axial planes in a 3-D image, a novel method was presented in this study to explain the relativity among different structures in a stereo space. A straight line and a plane can be defined by two and three points respectively in a stereo space. Some specific mark points are recognizable in distal tibia. So this method was also used in this study. Surface shaded display was applied. It was the first 3-D rendering technique applied to medical imaging and was mainly applied in orthopaedics because of its superiority for bony surface reconstructions [15-17]. Besides, the distinct surfaces can facilitate clinical measurements [18]. In addition, it is rather difficult to collect a large sample of cadaver specimens. The morphological measurement on 3-D CT post processing images can be based on a large sample size and thus provide a more reliable and accurate data set.

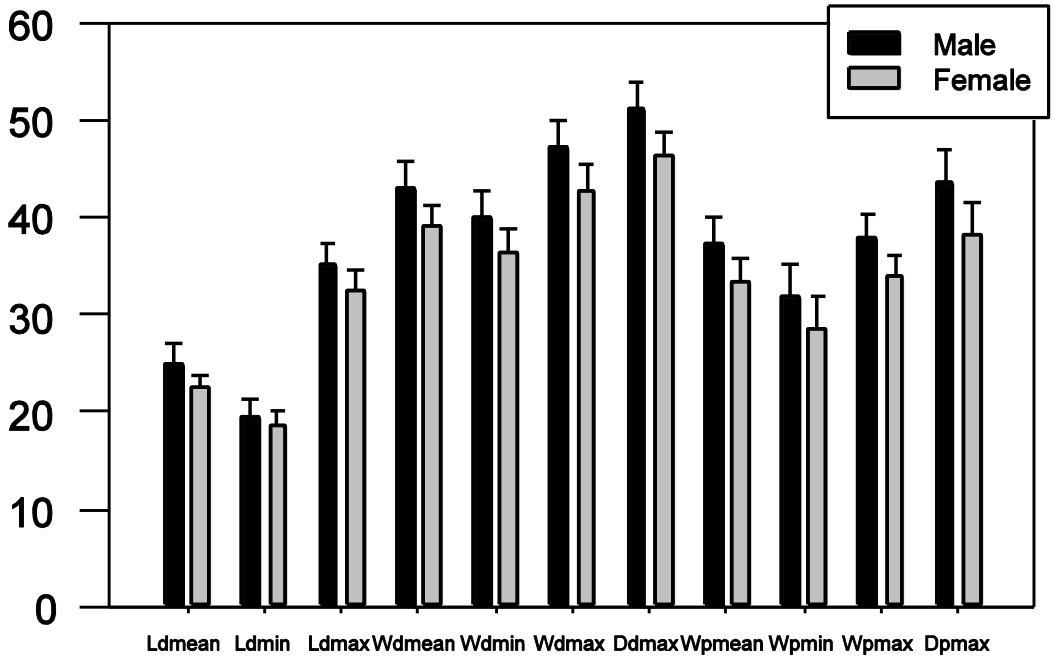

FIGURE 5 Significant differences were observed in all parameters between different genders (P<0.05)

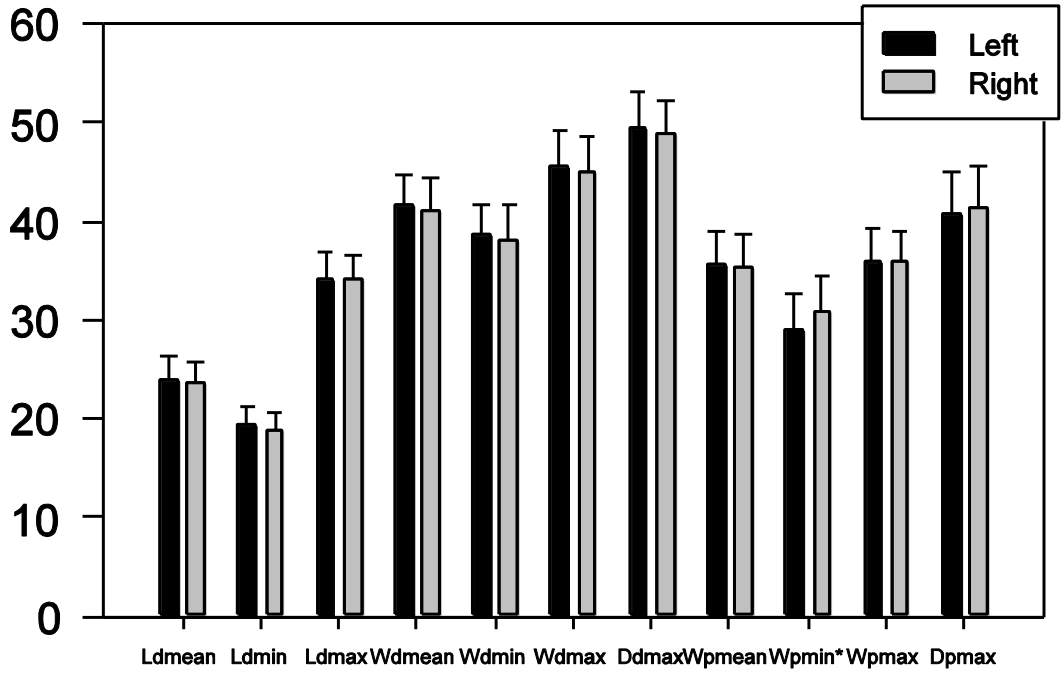

FIGURE 6 *Significant differences were observed in the minimum width on the level of the roof of the distal tibiofibular syndesmosis between left and right tibia (*P*<0.05)

The intra-observer and inter-observer reliability in this study are relatively high. It demonstrates that the values produced by three observers using 3-D CT post processing techniques are accurate and reproducible.

The dimensions of distal tibia offer guidance on the required screw length. As we all know, the length of implanted screws in the plane of distal tibia should be sufficient but no more than the maximum. Or exposed screw tail may stimulate and injure adjacent anatomic structures. If screws inserted were too long or too short, replacement and more fluoroscopy are inevitable. Frequent use of depth gauge, percutaneous insertion and replacement of screws, and poor implantation may lead to injury to nerves, vessels, tendons and articular surfaces. Many important anatomical structures are very close to distal tibia cortex. The anterior tibial compartment

contains tibialis anterior tendon, deep peroneal nerve, anterior tibial neurovascular bundle, the posterior includes tibialis posterior tendon, posterior tibial neurovascular bundle, and the lateral has tibiofibular syndesmosis [19]. Ali et al. [12] reported that the anterior neurovascular bundle was 3 mm from the anterior tibial

TABLE 1 Intra-observer and inter-observer reliability of all parameters

	Observer 1	Observer 2	Observer 3	ICC1	ICC2	ICC3	ICC12	ICC13	ICC23
Ldmean (mm)	23.77 ± 2.19	23.96 ± 2.12	23.76 ± 2.11	0.98	0.98	0.97	0.97	0.98	0.98
Ldmin (mm)	19.08 ± 1.80	19.20 ± 1.85	19.15 ± 1.78	0.90	0.93	0.91	0.95	0.97	0.96
Ldmax (mm)	34.05 ± 2.61	34.26 ± 2.49	33.96 ± 2.56	0.91	0.92	0.92	0.91	0.91	0.90
Wdmean (mm)	41.72 ± 3.29	41.22 ± 3.59	41.26 ± 2.98	0.96	0.72	0.95	0.83	0.81	0.84
Wdmin (mm)	38.67 ± 3.38	38.18 ± 3.43	38.29 ± 3.30	0.92	0.95	0.95	0.90	0.82	0.93
Wdmax (mm)	45.73 ± 3.58	45.25 ± 3.73	44.90 ± 3.67	0.92	0.95	0.87	0.91	0.89	0.90
Ddmax (mm)	49.56 ± 3.61	48.98 ± 3.70	49.05 ± 3.34	0.90	0.93	0.95	0.93	0.87	0.91
Wpmean (mm)	35.87 ± 3.43	35.55 ± 3.42	35.07 ± 3.21	0.95	0.97	0.94	0.96	0.93	0.95
Wpmin (mm)	30.46 ± 4.13	30.04 ± 3.75	30.34 ± 3.44	0.93	0.95	0.96	0.92	0.89	0.94
Wpmax (mm)	35.71 ± 2.95	36.19 ± 3.36	35.94 ± 3.27	0.77	0.94	0.94	0.88	0.87	0.95
Dpmax (mm)	41.29 ± 4.63	40.99 ± 4.38	40.85 ± 4.14	0.72	0.97	0.97	0.89	0.87	0.96

Ldmean: mean anteroposterior length on the distal plane (base of the distal tibiofibular syndesmosis), Ldmin: minimum length on the distal plane, Ldmax: maximum length on the distal plane, Wdmean: mean medial-lateral width on the distal plane, Wdmin: minimum width on the distal plane, Wdmax: maximum width on the distal plane, Ddmax: maximum diagonal on the distal plane, Wpmean: mean width on the proximal plane (roof of the distal tibiofibular syndesmosis), Wpmin: minimum width on the proximal plane, Wpmax: maximum width on the proximal plane, Dpmax: maximum diagonal on the proximal plane

ICC1, ICC2, ICC3: intraclass correlation coefficient for the first, second and third observer, ICC12, ICC13, ICC23: interclass correlation coefficient between the first and second, between the first and third and between the second and third observer, respectively

Reliability is excellent if ICC is greater than or equal to 0.75, moderate if between 0.4and 0.74, poor if less than or equal to 0.4

cortex and the posterior cortex was 1 mm from the tibialis posterior tendon and 3 mm to the posterior neurovascular bundle. Iatrogenic injury may occur during surgical manoeuvres for insertion of the screws including incision, blunt dissection down to the plate, drilling screw holes and finally the insertion itself [11]. Deangelis et al. [20] found the superficial peroneal nerve to be at significant risk during percutaneous screw placement in distal tibia. Bono et al. [10] found a relatively high incidence of about 63% of at least one structure damage after anteroposterior locking bolts inserted into the distal metaphyseal tibia. According to our results, from medial to lateral margin, the anteroposterior length increase from 19.65 mm and 18.52 mm to 35.35 mm and 32.53 mm in male and female at the level of the base of the tibiofibular syndesmosis respectively. The screws would probably penetrate the far cortex and injure the structures surrounding the distal tibia if longer than 35.35 mm and 32.53 mm in male and female (Figures 1 and 2). The results of this study present a possibility for surgeons to estimate the length of screws before operation.

Special attention needs to be paid to avoid any disruption of the ankle syndesmosis, which is a joint between the distal tibia and fibula [21, 22]. The distal fibula can be rotated externally and translated postero-medially by an external rotation force [23]. And with ankle dorsiflexion, the distal fibula moves proximally, posteriorly and rotates externally [22]. There is a small area where the tibia and fibula are in direct contact at the base of the syndesmosis [14, 24]. Moreover, the width of the distal tibiofibular syndesmosis 9-12 mm proximal to the tibial plafond was 2-4 mm [13]. Therefore, only a small gap exists in the distal tibiofibular syndesmosis [5, 13, 14]. On both proximal and distal planes of tibiofibular syndesmosis, the medial-lateral width increases from posterior to anterior margin. On distal plane, from posterior to anterior margin, the mean medial-lateral widths increase from 40.03 mm and 36.33 mm to 47.29 mm and 44.22 mm in male and female respectively. Similarly, on distal plane, the widths increase from 31.80 mm and 28.64 mm to 37.82 mm and 33.92 mm. The screws should not longer than the maximum diagonals which are 51.29 mm and 46.58 mm on distal plane and 43.64 mm and 38.24 mm on proximal plane in male and female respectively, or inadvertent distal tibiofibular syndesmosis penetration may occur (Figure 2).

However, the extent of distal tibiofibular syndesmosis is not clearly defined [14]. Kelikian et al. [21] postulated that the distal tibiofibular syndesmosis begins at the level of origin of the tibiofibular ligaments from the tibia and ends where these ligaments insert into the fibular malleolus. The anterior tibiofibular ligament originates close above the anterior tubercle of the distal tibia and the posterior ligament extends from the posterior tibial malleolus [14, 24]. The anterior tubercle is larger than the posterior tubercle [14]. In addition, it is sometimes difficult to distinguish between the proximal margin of the posterior tibiofibular ligament and the interosseous tibiofibular [24]. Therefore, the proximal margin of the anterior tubercle of the tibia was defined as the roof of the tibiofibular syndesmosis.

We acknowledge there are some limitations of the study. The cross-sections in this study were defined by several points. Therefore, the measured values may be

inconsistent with those measured by two-dimensional MRI scans and CT scans. Moreover, there is no clear statement about the exact extent of the tibiofibular syndesmosis [14]. In this study, the plane through the most proximal point of the anterior tubercle was defined as the most proximal extent of the joint, which worthy of continuous further study and improvement. Further clinical results are needed to test the findings of the study.

5 Conclusion

The study provides 3-D CT post processing techniques-based detailed values of distal tibia. The dimensions of distal tibia offer guidance on the required screw length. The anteroposterior length increases from medial to lateral margin at the level of the base of the tibiofibular syndesmosis. On both proximal and distal planes of tibiofibular syndesmosis, the medial-lateral width increases from posterior to anterior margin. The anteroposterior screws would probably penetrate the far cortex and injure the structures surrounding the distal tibia if longer than 35.35 mm and 32.53 mm in male and female. The screws should not longer than the maximum diagonals which are 51.29 mm and 46.58 mm on distal plane and 43.64 mm and 38.24 mm on proximal plane in male and female respectively, or inadvertent distal tibiofibular syndesmosis penetration may occur.

Acknowledgments

This study was supported by the National Natural Science Foundation of China (81000818, 81271989 and 81370053)

References

[1] Mandracchia V J, Evans R D, Nelson S C, Smith K M 1999 Pilon fractures of the distal tibia *Clin Podiatr Med Surg* **16**(4) 743-67
[2] Ristiniemi J 2007 External fixation of tibial pilon fractures and fracture healing *Acta Orthop Suppl* **78**(326) 3, 5-34
[3] Singer B R, McLauchlan G J, Robinson C M, Christie J 1998 Epidemiology of fractures in 15,000 adults: the influence of age and gender *J Bone Joint Surg Br* **80**(2) 243-8
[4] Hasenboehler E, Rikli D, Babst R 2007 Locking compression plate with minimally invasive plate osteosynthesis in diaphyseal and distal tibial fracture: a retrospective study of 32 patients *Injury* **38**(3) 365-70
[5] Khoury A, Liebergall M, London E, Mosheiff R 2002 Percutaneous plating of distal tibial fractures *Foot Ankle Int* **23**(9) 818-24
[6] Redfern D J, Syed S U, Davies S J 2004 Fractures of the distal tibia: minimally invasive plate osteosynthesis *Injury* **35**(6) 615-20
[7] Ronga M, Longo U G, Maffulli N 2010 Minimally invasive locked plating of distal tibia fractures is safe and effective *Clin Orthop Relat Res* **468**(4) 975-82
[8] Sitnik A A, Beletsky A V 2013 Minimally Invasive Percutaneous Plate Fixation of Tibia Fractures: Results in 80 Patients *Clin Orthop Relat Res* **471**(9) 2783-9
[9] Mehlman C T, DiPasquale T G 1997 Radiation exposure to the orthopaedic surgical team during fluoroscopy: "how far away is far enough?" *J Orthop Trauma* **11**(6) 392-8
[10] Bono C M, Sirkin M, Sabatino C T, Reilly M C, Tarkin I, Behrens F F 2003 Neurovascular and tendinous damage with placement of anteroposterior distal locking bolts in the tibia *J Orthop Trauma* **17**(10) 677-82
[11] Pichler W, Grechenig W, Tesch N P, Weinberg A M, Heidari N, Clement H 2009 The risk of iatrogenic injury to the deep peroneal nerve in minimally invasive osteosynthesis of the tibia with the less invasive stabilisation system: a cadaver study *J Bone Joint Surg Br* **91**(3) 385-7
[12] Ali A A, Gregory J J, Ockenden M, Hill S O, Makwana N K 2012 Anatomic description of the distal tibia: implications for internal fixation *J Foot Ankle Surg* **51**(3) 296-8
[13] Elgafy H, Semaan H B, Blessinger B, Wassef A, Ebraheim N A 2010 Computed tomography of normal distal tibiofibular syndesmosis *Skeletal Radiol* **39**(6) 559-64
[14] Hermans J J, Beumer A, de Jong T A, Kleinrensink G J 2010 Anatomy of the distal tibiofibular syndesmosis in adults: a pictorial essay with a multimodality approach *J Anat* **217**(6) 633-45
[15] Chen Y X, Lu X L, Bi G, Yu X, Hao Y L, Zhang K, Zou L L, Mei J, Yu G R 2011 Three-dimensional morphological characteristics measurement of ankle joint based on computed tomography image post-processing *Chin Med J Engl* **124**(23) 3912-8
[16] Zhang K, Chen Y X, Qiang M F, Li H B, Dai H 2014 The morphology of medial malleolus and its clinical relevance *Pak J Med Sci* **30**(2) 348-51
[17] Chen Y X, Zhang K, Hao Y N, Hu Y C 2012 Research status and application prospects of digital technology in orthopaedics *Orthop Surg* **4**(3) 131-8
[18] Kuszyk B S, Heath D G, Bliss D F, Fishman E K 1996 3-D CT: advantages of volume rendering over surface rendering *Skeletal Radiol Skeletal* **25**(3) 207-14
[19] Davidovitch R I, Egol K A 2010 *Rockwood & Green's fractures in adults* (7th edition) ed Bucholz RW, Heckman JD, Court-Brown CM and Tornetta P Lippincott Williams & Wilkins,Philadelphia PA, United States pp 1993-5
[20] Deangelis J P, Deangelis N A, Anderson R 2004 Anatomy of the superficial peroneal nerve in relation to fixation of tibia fractures with the less invasive stabilization system *J Orthop Trauma* **18**(8) 536-9
[21] Kelikian H and Kelikian A S 1985 *Disorders of the ankle* Saunders: Philadelphia
[22] Pena F A, Coetzee J C 2006 Ankle syndesmosis injuries *Foot Ankle Clin* **11**(1) 35-50, viii
[23] Beumer A, Valstar E R, Garling E H, Niesing R, Ranstam J, Löfvenberg R, Swierstra B A 2003 Kinematics of the distal tibiofibular syndesmosis: radiostereometry in 11 normal ankles *Acta Orthop* **74**(3) 337-43
[24] Bartonicek J 2003 Anatomy of the tibiofibular syndesmosis and its clinical relevance *Surg Radiol Anat* **25**(5-6) 379-86

Authors

Kun Zhang, born on November 3, 1988, Jiangsu, China

Current position, grades: Resident Doctor
University studies: Tongji Unversity, Shanghai, China
Scientific interest: Traumatic orthopaedics, foot and ankle surgery, computer-assisted orthopaedic surgery
Publications: 2 papers were indexed by SCI
Experience: Graduated from Tongji Unversity School of Medicine, has 3-year clinical experience in the field of traumatic orthopaedics, foot and ankle surgery and computer-assisted orthopaedic surgery.

Yanxi Chen, born on November 20, 1975, Chongqing, China

Current position, grades: Associate Chief Doctor
University studies: Tongji Unversity, Shanghai, China
Scientific interest: Traumatic orthopaedics, foot and ankle surgery, computer-assisted orthopaedic surgery
Publications: 7 papers were indexed by SCI
Experience: Associate professor, MD, ph.D, has a high reputation in the field of traumatic orthopaedics, foot and ankle surgery and computer-assisted orthopaedic surgery in China; Member of the Société Internationale de Chirurgie Orthopédique et de Traumatologie (SICOT).

Minfei Qiang, born on September 15, 1989, Shanghai, China

Current position, grades: Resident Doctor
University studies: Tongji Unversity, Shanghai, China
Scientific interest: Traumatic orthopaedics, foot and ankle surgery, computer-assisted orthopaedic surgery
Publications: 2 papers were indexed by SCI
Experience: Graduated from Tongji Unversity School of Medicine, has 3-year clinical experience in the field of traumatic orthopaedics, foot and ankle surgery and computer-assisted orthopaedic surgery.